

## CORE-POLARIZATION EFFECTS ON THE MAGNETIC TRANSITIONS IN THE $^{208}\text{Pb}$ REGION

I. HAMAMOTO<sup>1,2</sup>

*Center for Theoretical Physics, Laboratory for Nuclear Science,  
and Department of Physics, MIT, Cambridge, MA 02139, USA*

J. LICHTENSTADT<sup>2</sup>

*Bates Linear Accelerator Center, Laboratory for Nuclear Science,  
and Department of Physics, MIT, Cambridge, MA 02139, USA*

and

G.F. BERTSCH<sup>3</sup>

*Department of Physics and Cyclotron Laboratory, Michigan State University,  
East Lansing, MI 48824, USA*

Received 25 February 1980

We show that there is a reduction of the magnetic transition strength at high momentum transfer due to core polarization. This accounts substantially for the observed reduction of 50% of the  $J^\pi = 12^-$  and  $14^-$  transitions in  $^{208}\text{Pb}$ . The core polarization does not affect the shape of the high  $J$  form factors in the vicinity of their main peaks. However, a significant  $q$ -dependent effect is predicted for the ground state M1 moment of  $^{207}\text{Pb}$ .

High spin states with unnatural parity of  $J^\pi = 14^-$  (6.74 MeV) and  $12^-$  (6.43 and 7.06 MeV) have been measured recently in inelastic electron scattering measurements indicating significant reduction from the single particle-hole predictions [1]. The observed strengths around the first maximum of the form factors were only about 50% of the predictions from the  $\nu(1j_{15/2}, 1i_{13/2}^{-1})14^-$ ,  $12^-$  and the  $\pi(1i_{13/2}, 1h_{11/2}^{-1})12^-$  configurations. The purpose of the present letter is to estimate the core-polarization effect on these magnetic form factors, by using the technique of integrating the Schrödinger equation in the radial coordinate space<sup>†1,2</sup>.

Since in each of these high spin states one definite particle-hole configuration (denoted by  $p_0-h_0$ ) is supposed to be the overwhelmingly predominant component, we calculate the contributions from the graphs shown in figs. 1a and 1b. The complete sum over particle-hole configurations  $p, h$  may be performed easily if the residual interaction is approximated by a delta function. We obtain the following inhomogeneous equation [2-4] for the perturbed particle wavefunction,  $X_{ph}(r)$ ,

$$\left\{ \frac{\hbar^2}{2m} \left( -\frac{d^2}{dr^2} + \frac{l_p(l_p+1)}{r^2} \right) + V(r) - (E + \epsilon_h) \right\} rX_{ph}(r) \\ = -rR_{h_0}(r)R_h(r)R_{p_0}(r)((Y_{l_p \frac{1}{2}})^{j_p}(Y_{h \frac{1}{2}})^{j_h}|v\delta(\Omega_1 - \Omega_2)|)(Y_{l_{p_0} \frac{1}{2}})^{j_{p_0}}(Y_{h_0 \frac{1}{2}})^{j_{h_0}}\rangle_J. \quad (1)$$

<sup>1</sup> Address after September 1980: Nordita, Copenhagen, Denmark.

<sup>2</sup> Supported in part by US DOE, contract No. EY-76-C-02-3069.

<sup>3</sup> Supported in part by the National Science Foundation.

<sup>†1</sup> This formalism was taken from Buck and Hill [2]. See also Hamamoto [3].

<sup>†2</sup> It is useful both formally and numerically to define a Green's function here. See Shlomo and Bertsch [4].

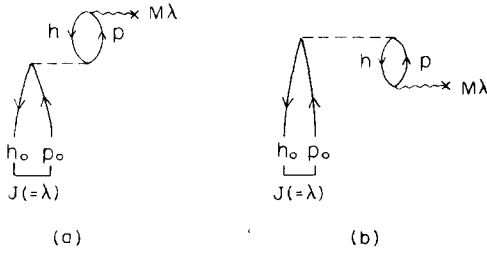


Fig. 1. Core polarization diagrams which are included in present calculations.

Here  $E$  is the excitation energy of the state,  $R(r)$  is the radial wavefunction and  $V(r)$  is the single-particle potential which we take to have the usual Woods–Saxon form<sup>†3</sup>. We include only the direct matrix element of the  $\delta$ -function residual interaction in eq. (1); the strength of the interaction will be discussed below. The perturbed particle wavefunctions  $X_{ph}(r)$  have a normalization given by the probability of that amplitude in the complete wavefunction. The particle amplitude for fig. 1b, denoted by  $Y_{ph}(r)$ , is obtained by changing the sign of  $E$  in eq. (1). As computed by eq. (1) the  $X_{ph}$  may contain components below the Fermi sea. These are easily projected out and we have done so, but in fact the observables are unaffected by this projection [4].

The experiment measures the magnetic form factor,

$$|F_{MJ}(q)|^2 = \frac{d\sigma}{d\Omega}_{\text{Mott}} \frac{1}{(\frac{1}{2} + \tan^2 \frac{1}{2}\theta)} \frac{1}{\eta}, \quad \left. \frac{d\sigma}{d\Omega} \right|_{\text{Mott}} = \frac{Z^2 \alpha^2}{q^2 \tan^2 \frac{1}{2}\theta}, \quad (2)$$

with the recoil factor:  $\eta = [1 + (2E_e/M_t) \sin^2 \frac{1}{2}\theta]^{-1}$ . In the Born approximation the form factor is related to the magnetic transition density  $\tilde{\rho}_{JJ}(r)$ :

$$F_{MJ}(q) = \frac{\sqrt{4\pi}}{Z} \left( \frac{2J_f + 1}{2J_i + 1} \right)^{1/2} \int r^2 dr j_f(qr) \tilde{\rho}_{JJ}(r). \quad (3)$$

The magnetic transition density (before including corrections due to the finite size of the nucleon) can be written as [5]

$$\rho_{JJ}(r) = \frac{\hbar}{2mc} \frac{1}{\sqrt{2J_f + 1}} \sum_{\pm} \left( \frac{J + \frac{1}{2} \mp \frac{1}{2}}{2J + 1} \right)^{1/2} \left[ (J + \frac{1}{2} \pm \frac{3}{2}) \frac{\mu_{\pm}^J(r)}{r} \pm \frac{d\mu_{\pm}^J(r)}{dr} \right], \quad (4)$$

with

$$\mu_{\pm}^J = (\mu_{\pm}^J)_0 + \delta\mu_{\pm}^J,$$

$$(\mu_{\pm}^J)_0 = 2R_{p_0}(r)R_{h_0}(r)\langle j_{p_0} \| \left[ Y_{J\pm 1} \left( \frac{g_l}{J + \frac{1}{2} \mp \frac{1}{2}} l \mp \mu s \right) \right]_{(J\pm 1, 1)J} \| j_{h_0} \rangle,$$

$$\delta\mu_{\pm}^J = 2 \sum_{ph \neq p_0 h_0} [X_{ph}(r) + Y_{ph}(r)] R_h(r) \langle j_p \| \left[ Y_{J\pm 1} \left( \frac{g_l}{J + \frac{1}{2} \mp \frac{1}{2}} l \mp \mu s \right) \right]_{(J\pm 1, 1)J} \| j_h \rangle, \quad (5)$$

$\mu^{\pi} = 2.79$ ,  $\mu^{\nu} = -1.91$ . Contributions from the convection and the magnetization current densities were folded with the respective nucleon charge and magnetization densities [6]. The folded densities were then used to cal-

<sup>†3</sup> Woods–Saxon radial parameters were not adjusted to fit the data. A standard set of parameters from ref. [12] was used in the numerical calculation.

culate the  $(e, e')$  cross sections in the distorted wave Born approximation (DWBA) [7].

The strength of the  $\delta$ -function interaction is written with four independent spin-isospin components:

$$v = v_0 + v_\tau \tau_1 \cdot \tau_2 + v_\sigma \sigma_1 \cdot \sigma_2 + v_{\sigma\tau} \sigma_1 \cdot \sigma_2 \tau_1 \cdot \tau_2. \quad (6)$$

The direct matrix element of (6), as in fig. 1a, is the approximation to the sum of the direct and exchange parts of the true residual interaction. Since we deal here with spin-flip transitions we need only to consider the  $v_\sigma$  and  $v_{\sigma\tau}$  components of the effective interaction. These components are not very well known especially at high momentum transfer. One way to fix this strength is to use the  $T$ -matrix approximation. Here the strength of the  $\delta$ -function is given by

$$v_i = -(4\pi\hbar^2/m) \operatorname{Re} f_i, \quad (7)$$

where  $f_i$  is a free nucleon-nucleon scattering amplitude. Calculation of  $f$  with a standard set of phase shifts yields<sup>†4</sup>

$$f_\sigma^{\text{nn}} = -0.30 - 0.14i \text{ fm}, \quad f_\sigma^{\text{np}} = -0.09 + 0.10i \text{ fm}. \quad (8)$$

In view of the relatively small magnitude of  $f_\sigma^{\text{np}}$ , we shall neglect the neutron-proton interaction. This is also supported by the SU(4) symmetry. The strength of the identical particle interaction,  $v_\sigma^{\text{nn}} = v_\sigma + v_{\sigma\tau}$ , as given by eq. (7) is shown in table 1.

Another way to fix the strength of the interaction is to fit the energy shifts of the particle-hole states. Empirically, the  $14^-$  state is shifted upward by 0.26 MeV from the particle-hole energy of the particle-hole state. The value obtained for  $v_\sigma^{\text{nn}}$  by fitting this energy shift is smaller than the  $T$ -matrix estimate as may be seen in table 1. In comparison the value obtained in ref. [10] which fits the static M1 moment is about four times larger. We adopted in our calculations the value  $v_\sigma^{\text{nn}} = 170 \text{ MeV fm}^3$ . Despite some ambiguity in the overall strength, the calculation should be reliable as to the shape of the polarization effect.

The residual interaction with the adopted strength produces substantial core polarization effects. In an infinite system the polarization is readily calculated with the Lindhard function,  $U$  [11],

$$\langle \delta\sigma \rangle / \langle \sigma \rangle = -2v_\sigma^{\text{nn}} (mk_F / 2\pi^2 \hbar^2) U(q, \omega), \quad U(0, 0) = 1.$$

In our case of nearly static polarization at maximum momentum transfer across the Fermi surface ( $\omega \approx 0$ ,  $q \approx 2k_F$ ), the values  $U(2k_F, 0) = \frac{1}{2}$  and  $v_\sigma^{\text{nn}} = 170$  yield a polarization  $\langle \delta\sigma \rangle / \langle \sigma \rangle = -0.28$ , which is close to what we obtained from the detailed calculation with eqs. (1)–(6).

Comparison between the calculated transition densities with and without core polarization for the  $14_\nu^-$  and the  $12_\pi^-$  are shown in fig. 2. The respective calculated  $(e, e')$  cross sections are also compared with the measured data<sup>†3</sup>. The calculated cross sections which are reduced due to core polarization agree rather well with the measured data both in the absolute magnitude and in the  $q$  dependence.

Other effects which may also cause a reduction in the transition strength were not considered here. One of

<sup>†4</sup> The scattering matrix corresponding to spin-flip of the stretched  $j = l + \frac{1}{2}$  configurations is  $2f_\sigma = \langle k = k_F \hat{z}, \rightarrow \leftarrow | M | k = -k_F \hat{z}, \leftarrow \rightarrow \rangle = -\frac{1}{2} M_{88}(\pi) + \frac{1}{2} M_{11}(\pi)$ , in the notation of Stapp et al. [8]. We evaluate this at  $E_{\text{cm}} = 70 \text{ MeV}$  using the phase shifts of McGregor et al. [9].

Table 1  
Strength of the spin-flip interaction for identical particles.

Method	$v_\sigma^{\text{nn}}$ (MeV fm <sup>3</sup> )
$T$ -matrix, eq. (7)	156
$14^-$ shift = 0.26 MeV	115
Ref. [10]	493
Adopted	170

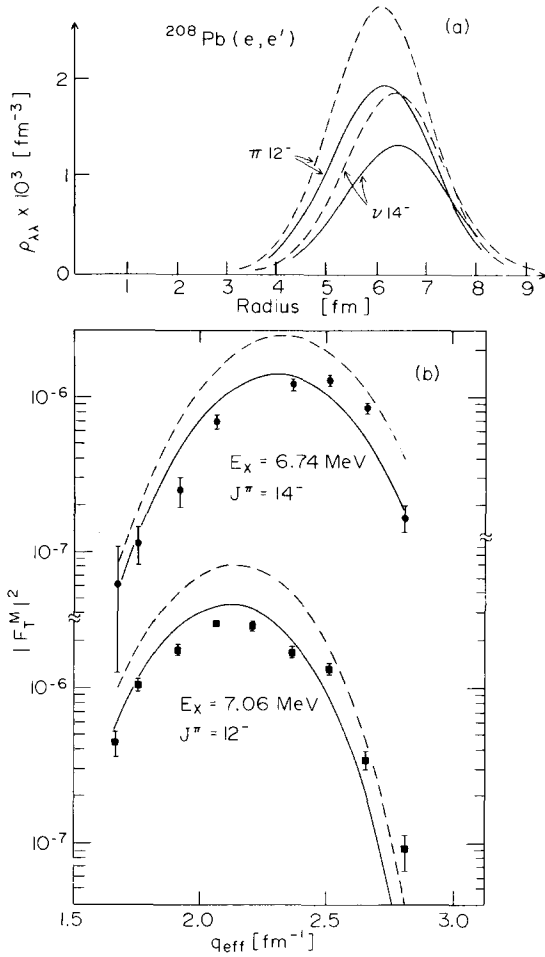


Fig. 2. (a) Magnetization current densities for the  $\nu 14^-$  and the  $\pi 12^-$  transitions in  $^{208}\text{Pb}$ . (b) Transverse (e, e') form factors calculated in DWBA from the densities in (a), compared to the  $160^\circ$  data of ref. [1].  $q_{\text{eff}} = q(1 + 4Z\alpha/3EA^{1/3})$ . In both (a) and (b) the dashed lines are the calculations for the unperturbed single particle-hole configuration, while solid lines are the calculations including core polarization. A standard set of Woods-Saxon potential parameters [12] are used in the numerical calculations.

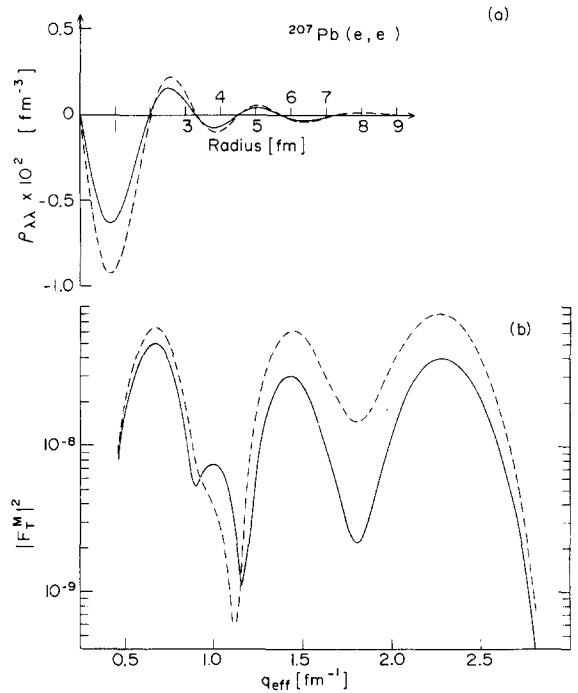


Fig. 3. Magnetization current density and the respective DWBA (e, e) form factor of the M1 in  $^{207}\text{Pb}$ . Dashed lines are the unperturbed single particle calculations, while solid lines are the calculations including core polarization.

these can be related to the fact that the high  $j$  single particle states in the  $^{208}\text{Pb}$  region are not pure "shell model" states. Namely the neutron  $1j_{15/2}$  and  $1i_{13/2}$  states and the proton  $1i_{13/2}$  and  $1h_{11/2}$  are known to have appreciable admixtures of the octupole ( $3^-$ ) core excitation ( $\approx 2.6$  MeV) [12]. Enhanced E3 decay of the  $1j_{15/2}$  state at 1.43 MeV to the  $2g_{9/2}$  ground state in  $^{209}\text{Pb}$  which was observed experimentally [13] is typical evidence for these admixtures. These "impurities" might also cause the (e, e') cross section to deviate from the one-particle--one-hole predictions. This deviation will be discussed elsewhere.

The calculated reduction discussed above seems to be almost constant and can be expressed approximately by a  $q$ -independent scaling factor, as can be seen for the  $12^-$  and the  $14^-$  states. This  $q$  independence is a feature

of the very high spin states obtainable from particle-hole configurations with one major shell excitation. For example, the reduction in  $14^-$  strength stems primarily from admixtures of configurations such as  $\nu(1k_{17/2}1h_{11/2}^{-1})14^-$ ,  $\nu(1l_{19/2}, 1i_{13/2}^{-1})14^-$  and the  $\nu(1l_{19/2}, 1g_{9/2}^{-1})14^-$ , all of which have similar radial dependence to that of the unperturbed  $\nu(1j_{15/2}, 1i_{13/2}^{-1})$  configuration. The resulting polarization effect which is concentrated around the nuclear surface is rather unique to the present high spin states.

A calculation of the polarization effect on the magnetic elastic scattering from  $^{207}\text{Pb}$  provides an excellent example which shows a different  $q$ -dependent behaviour. Since the spin of the  $^{207}\text{Pb}$  ground state is  $J^\pi = 1/2^-$ , M1 is the only multipole contributing to the elastic transverse form factor. It is a most favourable case for examining the magnitude of the M1 polarization in the very inside of the nucleus, since the unperturbed  $3p_{1/2}$  single particle wavefunction has there a large amplitude. We show in fig. 3 the calculated form factor with and without the polarization effect. The latter was calculated using the same technique described above with the same interaction used for the high spin states. It is seen from fig. 3 that around the momentum transfer of  $q = 1.0\text{--}2.5\text{ fm}^{-1}$  the predicted cross section is about one half of the pure single particle prediction. In this momentum transfer region the transition density at small radii is probed. It is noted that due to the unique feature [14] of the  $p_{1/2}$  single particle orbit together with the delta function interaction the calculated polarization vanishes in the limit  $q \rightarrow 0$ , giving rise to a magnetic moment which is equal to the Schmidt value. Preliminary measurements of elastic magnetic scattering from  $^{207}\text{Pb}$  around  $2.5\text{ fm}^{-1}$  show a significant reduction from the  $3p_{1/2}$  single particle prediction [15]. It would be very important to measure the elastic magnetic scattering from  $^{207}\text{Pb}$  up to high momentum transfer ( $\approx 2.5\text{ fm}^{-1}$ ). Since the M1 cross section remains rather large at this momentum transfer it should be measurable.

The polarization effect seems to be very important in the magnetic transitions to the high spin states, and can explain the major cause for the observed reduction from the single particle-hole predictions in  $^{208}\text{Pb}$ . The same effect predicts a  $q$ -dependent reduction of the M1 elastic form factor in  $^{207}\text{Pb}$  and measuring it would further test our approach. Similar quenching observed in other transverse form factors and examination of the dependence of the numerical results on the various parameters used in our calculations are still to be investigated. Other effects which contribute to the electron scattering cross section, such as meson exchange currents should be studied as well.

The authors would like to thank J. Heisenberg and A. Kerman for the helpful discussions. One of us (I.H.) would like to thank the Center for Theoretical Physics at MIT for its warm hospitality.

## References

- [1] J. Lichtenstadt et al., Phys. Rev. 20C (1979) 497.
- [2] B. Buck and A.D. Hill, Nucl. Phys. A95 (1967) 271.
- [3] I. Hamamoto, Phys. Lett. 66B (1977) 410; Proc. Intern. School of Physics Enrico Fermi, Course LXIX (1976) p. 258.
- [4] S. Shlomo and G.F. Bertsch, Nucl. Phys. A243 (1975) 507.
- [5] E.g. H.C. Lee, AECL 4839 Chalk-River, Ontario (1975), unpublished.
- [6] R. Hofstadter et al., Rev. Mod. Phys. 30 (1958) 482; W. Bertozzi et al., Phys. Lett. 41B (1972) 408.
- [7] J. Heisenberg, Code HEIMAG, unpublished.
- [8] H. Stapp, T. Ypsilantis and N. Metropolis, Phys. Rev. 105 (1957) 302.
- [9] M. McGregor, R. Arndt and R. Wright, Phys. Rev. 182 (1969) 1714.
- [10] P. Ring and J. Speth, Nucl. Phys. A235 (1974) 315.
- [11] J. Linhard, Dan. Vidensk. Selsk. Mat. Fys. Medd. (1954) no. 8.
- [12] E.g. I. Hamamoto, Phys. Rep. 10C (1974) 64.
- [13] C. Ellegaard, J. Kantele and P. Vedelsby, Phys. Lett. 25B (1967) 512.
- [14] H. Noya, A. Arima and H. Horie, Prog. Theor. Phys. 8 (1958) 33.
- [15] C.N. Papanicolas, Ph.D. Thesis, MIT (1979), to be published.